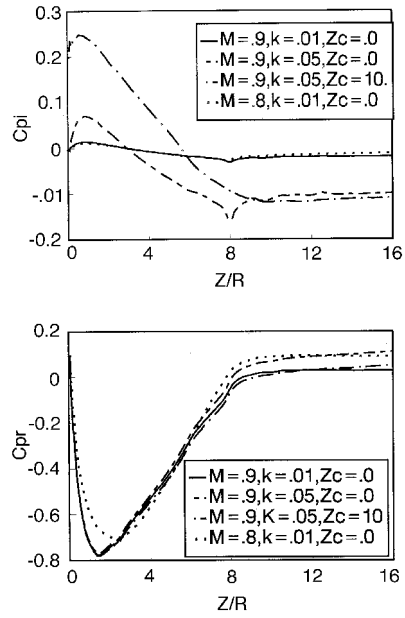

Fig. 3 Real and imaginary parts of unsteady surface pressure for a four-caliber ogive–nose–cylinder.

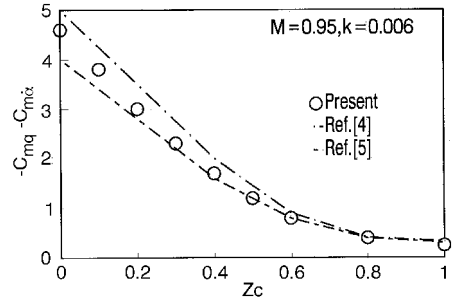

Fig. 4 Comparison of dynamic stability derivative vs pitching center for a parabolic arc nose.

frequency; it indicates a nonlinear dependence of the pitch-damping coefficient on reduced frequency. The conclusion is also suitable for the results with the variation of pitching center. For different Mach numbers (M = 0.8 and 0.9), the imaginary part is nearly unchanged, but the real part is changed, and the variations of the real part are similar to those of the quasisteady pressure.

No experimental data of dynamic stability derivatives are available for comparison. The dynamic derivative for a parabolic-arc nosed body are calculated by the present theory, and a comparison with results of the theory of Liu et al.[4] as well as Hsieh's[5] perturbation potential solution is made. The total damping-in-pitch coefficient versus pitching center is shown in Fig. 4. It indicates that the results of this theory have the same general tendency as Liu's and Hsieh's, but when the pitching center is close to the nose of the body, differences between the various theoretical appear. The result of the present theory lies between those of Liu's and Hsieh's theories. Therefore, the present theory seems equally capable of predicting dynamic stability derivatives.

Conclusions

A perturbation theory and numerical solution based on the unsteady Euler equations were developed for unsteady transonic flows about sharp-nosed bodies of revolution undergoing harmonic oscillations. The following conclusions can be drawn.

1) The quasisteady solution for the perturbation surface pressure for the sharp-nosed body of revolution agrees well with experimental results.

2) The unsteady results for a total damping-in-pitch coefficient agree well with results of the available calculation for a parabolic-arc nose. Although no experiment measurements for comparison are available, based on the analysis, the unsteady surface perturbation pressures are reasonable.

3) The theory is easily extended to treat three-dimensional unsteady flows on various configurations without limitation bodies of revolution. In engineering application, the theory may be efficient and effective for the prediction of unsteady flows and dynamic stability derivatives at small incidence.

Acknowledgments

The authors thank Zhuang Li-Xian, of the University of Science and Technology of China, for valuable discussions. The research was supported by the JSPS cooperation programs with southeast Asian countries under the core university system.

References

[1]Zhang, H., "Non-Oscillatory Containing No Free Parameter and Dissipative Scheme," *ACTA Aerodynamica Sinica*, Vol. 6, No. 2, 1989, pp. 145–155.

[2]Yoon, S., and Jameson, A., "An LU-SSOR Scheme for the Euler and Navier-Stokes equations," AIAA Paper 87-0600, Jan. 1987.

[3]Hartley, M. S., and Jacocks, J. L., "Static Pressure Distributions on Various Bodies of Revolution at Mach Numbers from 0.6 to 1.6," Arnold Engineering and Development Center, TR-68-37, March 1968.

[4]Liu, D. D., Platzer, M. F., and Ruo, S. Y., "Unsteady Linearized Transonic Flow Analysis for Slender Bodies," *AIAA Journal*, Vol. 15, No. 7, 1977, pp. 966–973.

[5]Hsieh, T., "Perturbation Solutions of Unsteady Transonic Flow over Bodies of Revolution," *AIAA Journal*, Vol. 16, No. 12, 1978, pp. 1271–1278.

Enhanced Multiobjective Technique for Multidisciplinary Design Optimization

John N. Rajadas,* Ralph A. Jury IV,†
and Aditi Chattopadhyay‡
Arizona State University, Mesa, Arizona 85206

Introduction

THE design of modern-day aircraft is a multidisciplinary process involving the integration of several disciplines such as aerodynamics, structures, dynamics, and propulsion, where optimization techniques that are able to address the different disciplines simultaneously are valuable tools. One such optimization technique is the Kreisselmeier–Steinhauser (K–S) function approach.[1] The K–S technique is a multiobjective optimization technique that combines all of the objective functions and the constraints to form a single unconstrained composite function that is then minimized using an appropriate unconstrained solver. The technique has been

Presented as Paper 97-0104 at the 35th Aerospace Sciences Meeting, Reno, NV, Jan. 6–9, 1997; received Sept. 8, 1997; revision received April 15, 1998; accepted for publication April 27, 1998.

*Department of Manufacturing and Aeronautical Engineering Technology. Senior Member AIAA.

†Department of Mechanical and Aerospace Engineering. Member AIAA.

‡Department of Mechanical and Aerospace Engineering. Associate Fellow AIAA.

shown to be effective in various applications such as tilt-rotor design, High-Speed Civil Transport (HSCT) design, wing design, sonic-boom minimization in HSCT, etc.[2,3] One of the characteristics of the K–S method is that all of the objective functions are equally weighted, which eliminates the need for user input in setting up the problem. However, in a realistic design application, it would be advantageous to have a method where a designer could emphasize specific design criteria relative to the others. In the present work, the K–S technique has been enhanced to provide such a capability by using weight factors that enable increased emphasis on specific objectives during the optimization process.[4]

Analysis

A general multiobjective optimization problem is minimize/maximize, $\boldsymbol{F}_k(\boldsymbol{\Phi})$, $k = 1, 2, \ldots, \mathrm{NF}$; subject to $\boldsymbol{g}_j(\boldsymbol{\Phi})$, $j = 1, 2, \ldots, \mathrm{NC}$, where $\boldsymbol{\Phi}$ is the design variable vector, $\boldsymbol{F}_k(\boldsymbol{\Phi})$ is the vector of objective functions, $g_j(\boldsymbol{\Phi})$ is the vector of constraints, and NF and NC are the number of objective functions and constraints, respectively. In the K–S technique, the original objective functions are transformed into reduced or normalized objective functions[1] that take on the following form:

$$\hat{f}_i(\phi) = \frac{F_i(\phi)}{F_{i_0}} - 1 - \boldsymbol{g}_{\max}, \qquad i = 1, 2, \ldots, \mathrm{NF}$$

where F_{i_0} represents the value of the original objective function at the current reference point, and F_i is its value calculated at the beginning of each iteration. $\boldsymbol{g}_{\max}$ is the largest of the constraint vectors and is held constant during each iteration. The reduced objective functions are analogous to the original constraints. Therefore, a new constraint vector $\boldsymbol{f}_m(\boldsymbol{\Phi})$, $m = 1, 2, \ldots, M$, where $M = \mathrm{NC} + \mathrm{NF}$, is introduced in which the first NC elements are the original constraints of the problem and the next NF elements are the reduced objective functions. The original constrained optimization problem with multiple objective functions is thus transformed into a single-objective, unconstrained minimization problem using the K–S function, as

$$F_{\mathrm{KS}}(\boldsymbol{\Phi}) = f_{\max} + \frac{1}{\rho}\log_e \sum_{m=1}^{M} \exp\{\rho[f_m(\boldsymbol{\Phi}) - f_{\max}]\}$$

where $f_{\max}$ is the largest constraint corresponding to the new constraint vector $\boldsymbol{f}_m(\boldsymbol{\Phi})$. The multiplier ρ, which is analogous to the drawdown factor of penalty function formulation, controls the distance from the surface of the K–S envelope to the surface of the maximum constraint function. When ρ is large the K–S function will closely follow the surface of the largest constraint function, and when ρ is small the K–S function will include contributions from all the constraints.[4] The new unconstrained minimization problem can be solved by using a variety of techniques. In the present work, the Broyden–Fletcher–Goldfarb–Shanno (BFGS) algorithm has been used.

The K–S approach has been enhanced by modifying the reduced objective functions using weight factors $\beta_i (i = 1, 2, \ldots, \mathrm{NF})$ as shown next:

$$\hat{f}_i(\phi) = \frac{\beta_i F_i(\phi)}{F_{i_0}} - \beta_i - g_{\max}, \qquad i = 1, \ldots, \mathrm{NF}$$

The weight factor β_i enables the designer to emphasize the ith objective function in the optimization problem. β_i are positive numbers whose numerical values are dictated by the specific application.

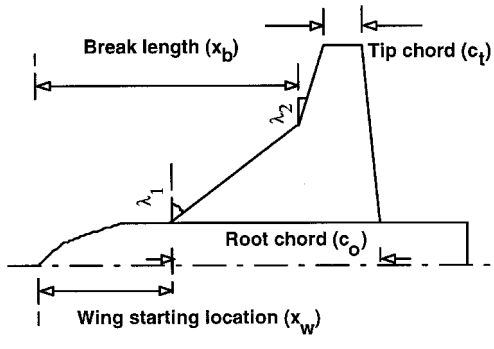

Fig. 1 HSCT configuration and design variables.

HSCT Sonic-Boom Application

The enhanced K–S technique has been demonstrated on a HSCT design (a doubly swept wing–body) for minimum sonic boom and improved aerodynamic performance (Fig. 1). A typical sonic-boom pressure signature exhibits two positive pressure peaks. The first peak (Δp_1) is a result of the bow shock around the nose of the aircraft and the second (Δp_2) is caused by the wing. Minimizing the extent of these pressure peaks is the main focus in the sonic-boom minimization problem. From an aerodynamics perspective, minimizing the drag to lift ratio (C_D/C_L) while maintaining the lift performance is important. In the present work, only the second pressure peak (Δp_2) and the C_D/C_L ratio have been used for the demonstration. The nose length and the maximum radius of the forebody were obtained for minimum Δp_1 and frozen at that level for the subsequent optimization of Δp_2 and C_D/C_L. The design variables for the optimization problem are shown in Fig. 1. The six design variables are wing root chord (c_0), the two leading-edge sweeps (λ_1 and λ_2), tip chord (c_t), break length (x_b), and wing starting location (x_w). Upper and lower bounds are imposed on these during the optimization process.

Results and Discussion

For the weighting factors the order of the objective functions (F_i) is C_D/C_L ($i = 1$), then the first and second pressure peaks ($i = 2, 3$). Thus, a (5,1,1) weight factor set indicates that C_D/C_L is weighted by a factor of 5 relative to Δp_1 and Δp_2. The "ref" indicates the configuration before the optimization process begins. As mentioned earlier, only the first and third objective functions will be assigned weighting factors. Table 1 summarizes the results of the demonstration using the enhanced K–S function technique. The effect of the weight factors on the objective functions are shown in Fig. 2, where the optimum solutions (after 24 cycles) obtained for unweighted [(1,1,1)], C_D/C_L-weighted [(5,1,1)] and $(\Delta p_2)_{\max}$-weighted [(1,1,10)] are compared with the reference values. There is excellent correlation between the weight factors and the optimized results. The results indicate that the enhanced K–S function technique is especially suited in a multidisciplinary design

Table 1 HSCT design variables

Design variables	Reference	(1,1,1)	(5,1,1)	(1,1,10)
First leading-edge sweep, λ_1, deg	70.46	73.76	74.11	73.93
Root chord, c_0 (m)	7.81	8.19	8.71	8.30
Second leading edge sweep, λ_2, deg	52.42	51.97	52.87	52.02
Tip chord, c_t, m	1.5776	1.2606	1.3439	1.2646
Break length, x_b, m	11.99	12.34	12.80	12.61
Wing starting location, x_w, m	7.80	7.59	7.50	7.77

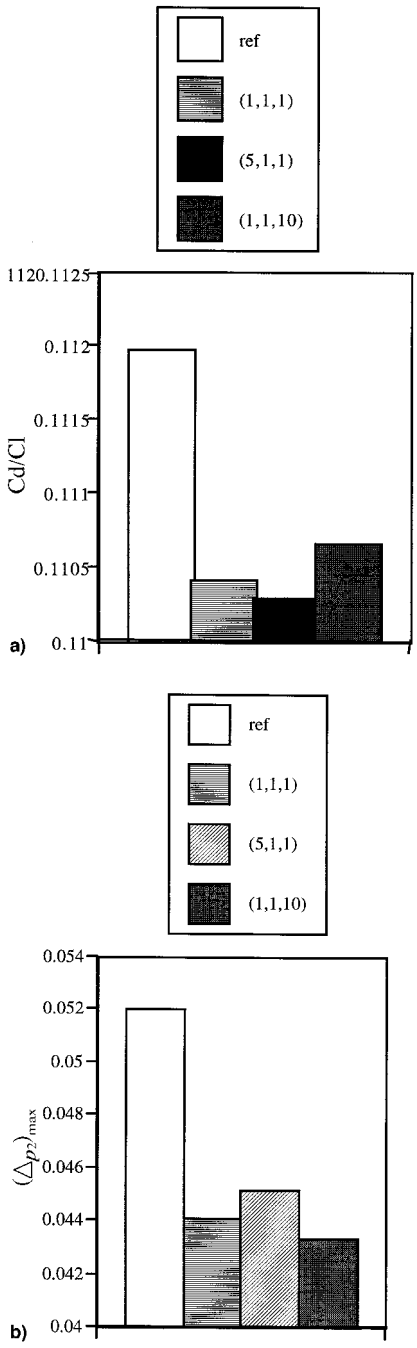

Fig. 2 Effect of weight factors on a) C_D/C_L and b) $(\Delta p_2)_{max}$.

application because of its ability to simultaneously address multiple objectives while incorporating the capability to emphasize specific objectives relative to the others. The procedure has been demonstrated, using a high-speed aircraft design problem, to be effective in achieving the desired goal of selectively emphasizing design objectives in the overall design process.

Acknowledgment

This work is sponsored by NASA Ames Research Center under Grant NCC2-5150.

References

[1]Wrenn, G. A., "An Indirect Method for Numerical Optimization Using the Kreisselmeier-Steinhauser Function," NASA CR 4220, 1989.

[2]McCarthy, T., Chattopadhyay, A., and Zhang, S., "A Coupled Rotor/Wing Optimization Procedure of High Speed Tilt-Rotor Aircraft," 51st Annual Forum of the American Helicopter Society, Fort Worth, TX, 1995.

[3]McCarthy, T., and Chattopadhyay, A., "Multidisciplinary Optimization of Helicopter Rotor Blades Including Design Variable Sensitivity," *Proceedings of the AIAA/USAF/NASA/OAI 4th Symposium on Multidisciplinary Analysis and Optimizations* (Cleveland, OH), 1992 (AIAA Paper 92-4750).

[4]Chattopadhyay, A., Jury, R. A., and Rajadas, J. N., "An Enhanced Multiobjective Formulation Technique for Multidisciplinary Design Optimization," AIAA Paper 97-0104, 1997.

Comparison of Aeroelastic Excitation Mechanisms

Rick Lind,* Lawrence C. Freudinger,† and David F. Voracek‡
NASA Dryden Flight Research Center, Edwards, California 93523-0273

Introduction

FLIGHT flutter testing relies heavily on measured aeroelastic flight data for safe and efficient envelope expansion. These data are used to determine the stability properties and predict the onset of flutter through algorithms to estimate damping parameters, transfer functions, and uncertainty descriptions for derived models.[1] The reliance on flight data presents a need for aeroelastic excitation mechanisms that can provide high levels of excitation across a wide range of frequencies. A recent AGARD conference identified such mechanisms as an important area of research for the aeroelastic and flight-test communities.[2]

This Note presents results from flight tests of the F/A-18 Systems Research Aircraft (SRA).[3] Flight data are recorded in response to three aeroelastic excitation mechanisms: atmospheric turbulence, pilot stick commands, and a wingtip exciter system. The performance of each mechanism is directly compared by analyzing power spectral information obtained from data recorded in response to each type of excitation at the same flight condition. This information demonstrates the level of excitation over a frequency range and the power of each modal response.

F/A-18 SRA

The F/A-18 SRA is being flown at NASA Dryden Flight Research Center as a testbed for flutter testing, advanced actuator concepts, smart structures, optical sensors and avionics systems. The SRA is a two-seat configuration fighter with production engines. Flutter testing was initiated on the SRA because of a major left wing structural modification to allow testing of several hydraulic and electromechanical aileron actuator concepts. The increased size and weight of these actuators required the replacement of a fitting called a *hinge-half* supporting the aileron hinge, the actuator, and a fairing with

Received May 31, 1997; revision received March 30, 1998; accepted for publication June 8, 1998.

*NRC Postdoctoral Research Fellow, Structural Dynamics Branch. E-mail: rick.lind@dfrc.nasa.gov. Member AIAA.

†Research Engineer, Structural Dynamics Branch. Member AIAA.

‡Research Engineer, Structural Dynamics Branch. Senior Member AIAA.